Fabrication & physicochemical characterization of *T. reesei* derived fungal chitosan-PVP blend membranes

Razi ur Rahman[1], Garima Mathur[1*]

[1]Centre of Excellence for Microbial and Plant Biotechnology, Department of Biotechnology, Jaypee Institute of Information Technology, A-10, Sector-62, Noida -201309, Uttar Pradesh, India

*Email: garimacity@gmail.com

Abstract

In this study, successful fabrication and characterization of fungal chitosan (FC)polyvinylpyrrolidone (PVP) blend membranes, derived from *Trichoderma reesei* MTCC 4876, are presented. The structural, chemical, and thermal characteristics of the fabricated FC-PVP blend membranes were systematically investigated by employing X-ray diffraction (XRD), Fouriertransform infrared (FTIR) spectroscopy, and differential scanning calorimetry (DSC) analyses, respectively. It was found that the membrane thickness varied from 0.01 mm for FC to 0.04-0.05 mm for blended membranes, depending on their composition and structural rearrangement. XRD data revealed a gradual change in membrane structure from semi-crystalline to amorphous with an increase in PVP content, while FTIR spectra clearly established strong intermolecular hydrogen bonding between -OH and -NH groups of chitosan and -C=O groups of PVP, resulting in better miscibility, homogeneity, and density of the blend membranes. From DSC data, it was evident that thermal stability and reduced crystallinity of FC-PVP blend membranes are superior to pure chitosan, indicating a stable and compatible polymer blend system. Thus, fungal chitosan blend membranes offer better flexibility, homogeneity, and stability, which make them promising materials for various biomedical, pharmaceutical, and environmentally friendly packaging materials.

Keywords- Fungal Chitosan, Polyvinylpyrrolidone, FTIR, XRD, DSC.

Introduction

Recently, there has been increasing interest in natural biopolymers as alternatives to synthetic materials because of their renewable sources, environmental safety, and versatile structures [1]. Among these, chitosan, derived from deacetylated chitin, is among the most studied and promising for multiple uses [2]. Chitin, the raw material for chitosan, is the second most common natural polymer after cellulose [3]. It is chiefly present in crustacean exoskeletons, insect shells, and fungal cell walls. Converting chitin to chitosan via alkaline deacetylation yields a cationic polymer with notable chemical features, including reactive amino and hydroxyl groups, variable molecular weight, and pH-dependent solubility [4]. These characteristics facilitate the production of chitosanbased membranes, films, nanoparticles, and hydrogels, thereby expanding its utility across materials science, biomedical engineering, and environmental applications [5].

Although the commercial sector has traditionally depended on chitosan extracted from crustaceans, chitosan derived from fungi has emerged as a potentially sustainable alternative, presenting several unique advantages [6]. The synthesis of fungal chitosan allows for enhanced control over consistency and quality this contrasts with chitosan sourced from crustaceans, which is subject to seasonal variations, geographical limitations, and the waste management difficulties associated with the seafood industry [7].

Fungal chitosan is extracted from fermentation processes, employing species like *Aspergillus niger*, *Mucor rouxii*, and *Rhizopus oryzae*, among others [8]. Consequently, this production method addresses the allergenic concerns linked to chitosan obtained from shellfish, thus making it appropriate for sensitive applications, including food packaging and biomedical devices [9]. Moreover, the regulated cultivation parameters result in chitosan with a more consistent chemical profile, degree of deacetylation, and molecular weight distribution, all of which are essential for reproducible membrane preparation and characterization [10].

Despite its many advantages, pure fungal chitosan films often have significant limitations. These include poor mechanical flexibility, brittleness, and high sensitivity to environmental factors like humidity and changes in pH [11]. To address these issues, blending chitosan with synthetic polymers has been broadly studied as an effective modification strategy [12]. Polyvinylpyrrolidone (PVP) is a polymer additive that has shown a good ability to work with chitosan matrices [13]. PVP, a biocompatible, non-ionic, and water-soluble polymer, is known for

its low toxicity, chemical stability, and excellent ability to form films [14]. Adding polyvinylpyrrolidone (PVP) to chitosan-based systems provides several benefits, such as increased mechanical strength, improved thermal stability, easier processing, and better resistance to environmental factors [15]. Furthermore, the inclusion of PVP increases the hydrophilicity of the material, which helps create a uniform solution for casting. As a result, the membranes created are more uniform and have better physical properties [16].

Solution casting is a common method for making polymer membranes, especially those that use chitosan-based composites [17]. This process involves dissolving the polymer components in a suitable solvent. The solvent is then evaporated in a controlled way, which leads to the formation of a continuous, solid membrane [18]. Critical factors that affect the final properties of the membrane, such as its shape, thickness uniformity, porosity, and mechanical performance, include polymer concentration, solvent choice, casting temperature, evaporation rate, and drying conditions [19]. Solution casting offers multiple benefits, such as being easy to use, reproducible, scalable, and cost-effective. This makes it useful for both research in the lab and making membranes on a large scale [20]. This method allows for precise control over membrane composition and thickness while keeping the polymer chains and their interactions intact [21]. Despite the increasing interest in chitosan-PVP composite membranes, numerous knowledge gaps persist in understanding the fundamental structure-property relationships in fungal chitosan-based systems. The majority of current research has concentrated on chitosan derived from crustaceans, resulting in insufficient exploration of the distinctive properties and behavior of fungal chitosanPVP composites [22]. A comprehensive understanding of the impact of PVP incorporation on the molecular interactions, crystalline structure, and thermal properties of fungal chitosan membranes is crucial for enhancing membrane performance and broadening their potential applications [23]. Our work aims to develop fungal chitosan-PVP membranes that could address current limitations in membrane technology while providing sustainable alternatives to conventional synthetic polymer membranes [24]. Such membranes hold significant potential for applications such as water treatment, food packaging, biomedical devices, and drug delivery systems [25]. Fungal chitosan has been previously extracted from *Trichoderma reesei* MTCC 4876 cultivated in submerged cultivation and was characterized using FTIR, DSC, spectroscopic

analysis, etc. [26]. Recovered FC-PVP blend membranes varying molar ratios were prepared by the solvent casting method and were characterized.

Experimental Material

Commercial chitosan with a degree of deacetylation >= 75.0% and Polyvinylpyrrolidone K30 (PVP) purchased from CDH Pvt. Ltd., India. All other chemicals used were of analytical grade.

Preparation of fungal chitosan-PVP blend membranes

The solution casting method was used to make the fungal chitosan-PVP blend (27). Fig 1 shows the solvent casting method in which Fungal chitosan was initially dissolved in 1 N acetic acid at different concentrations and stirred continuously at room temperature for five hours to ensure that it dissolved completely. After that, different amounts of PVP were added to the solution, and it was stirred constantly for 24 hours to mix it evenly. The mixture was spun at 3000 rpm for 15 minutes to get rid of air bubbles and any solid particles that hadn't dissolved. After that, the homogeneous solution was put into glass petri dishes and dried in a hot air oven at 50 °C for 12 hours. Once the film was dry, the films were carefully taken off the dishes, put in polybags, and kept in a desiccator until they were needed again. We were able to make blends with fungal chitosan-to-PVP ratios of 0.5:1, 0:1, 1:0.5, 1:1, 1:0, and CC 1:0.

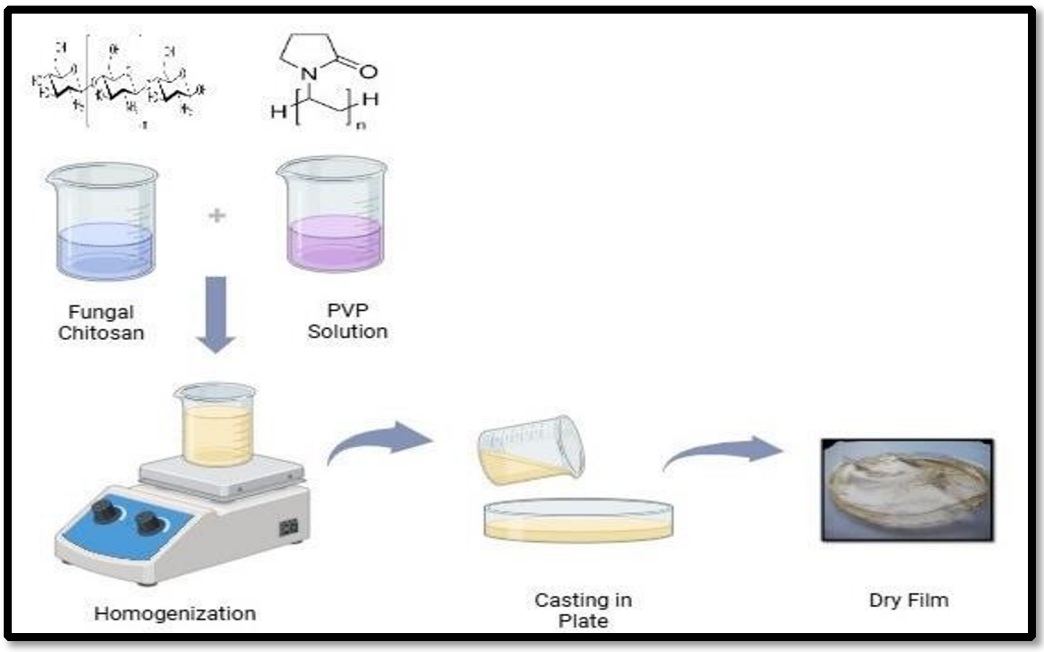

Figure 1. Solvent casting method for the preparation of CS: PVP blend membranes

Characterization of fungal chitosan -PVP blend membranes

Determination of the molecular weight of fungal chitosan

The viscosity-average molecular weight of fungal chitosan was determined using the Ostwald viscometric method (28). Chitosan, extracted from *Trichoderma reesei* was dissolved in a solvent system of 0.1 M acetic acid containing 0.2 M sodium chloride. A series of solutions with varying concentrations (e.g., 0.01, 0.02, 0.03, 0.04, and 0.05 g/dL) was prepared and allowed to equilibrate for 24 h at a controlled temperature of 25 ± 1 °C in a thermostatic water bath.

Flow times for the pure solvent (t_0) and each fungal chitosan solution (t) were measured using an Ostwald viscometer. The measurements were performed in triplicate for each sample, and the average flow time was used for calculations. The relative viscosity (η_r) was calculated as the ratio of the solution flow time to the solvent flow time ($\eta=t/t_0$). The specific viscosity (η_{sp}) was determined as ($\eta_{sp}=\eta_r-1$). Reduced viscosity (η_{red}) was then calculated by dividing the specific viscosity by the concentration (c), as shown in equation (1).

$$(\eta_{red})= \eta_{sp}/c \ldots\ldots\ldots (1)$$

The intrinsic viscosity (η) was obtained by plotting the reduced viscosity (η_{red}) versus the concentration (c) and extrapolating the linear trend line to zero concentration. The y-intercept of this plot yielded the value for intrinsic viscosity.

The viscosity-average molecular weight was subsequently calculated using the Mark–Houwink–Sakurada equation (2), where K and a are constants for a specific polymer-solvent-temperature system.

$$[\eta]=K.M^a \ldots\ldots\ldots (2)$$

Whereas a= 0.72 k= 4.74 dL/g

Determination of Blend Membrane Thickness

The thickness of the blend membrane was measured using a screw gauge. The average values of four random measurements were taken for each membrane thickness.

Visual inspection of the blend membranes

The membrane samples were analyzed with an optical microscopy Olympus BX 51, 10X amplification, to identify the presence of some imperfections, both after preparation and during storage. The uniformity of the blend membrane was assessed by cutting discs of 1 cm^2 from five different areas of the casted membrane samples.

Fourier Transform Infra-Red Spectroscopy (FT-IR)

Fourier-transform infrared spectroscopy (FTIR) is widely employed to study functional group interactions and to verify polymer blending. The fungal chitosan-PVP blend membranes were analyzed using an FT-IR spectrophotometer (Perkin Elmer Spectrum BX-II model) at Jaypee Institute of Information Technology, Noida. Measurements were carried out in transmission mode across the range of 4000-400 cm^{-1} with a spectral resolution of 4 cm^{-1}.

Differential Scanning Calorimetry (DSC)

The thermal characteristics of fungal chitosan-PVP blend membrane were examined using a differential scanning calorimeter (DSC, Hitachi DSC 7000X) at Jaypee Institute of Information Technology, Noida. Approximately 7 mg of the sample was sealed in an aluminium pan and subjected to heating from 30 °C to 500 °C at a constant rate of 2 °C per minute under a nitrogen atmosphere. An empty aluminium pan was used as the reference.

X-ray diffraction (XRD)

The crystalline properties of the fungal chitosan-PVP blend membrane were analyzed using X-ray diffraction (Shimadzu 600XRD) at Jaypee Institute of Information Technology, Noida. The dried samples were finely ground into powder form and mounted on an aluminium sample holder. Xray diffraction patterns were recorded with Cu-Kα radiation, scanning the samples in the range of 2θ = 5-30° at a speed of 2°/min.

Result and Discussion

The molecular weight of the extracted fungal chitosan was determined using the Ostwald viscometric method, which is based on the intrinsic viscosity of polymer solutions and the MarkHouwink-Sakurada equation. The calculated molecular weight was found to be 6.8×10^4 Da (6.8 kDa), indicating that the obtained chitosan falls within the range typically reported for fungalderived chitosan. Pochanavanich and Suntornsuk (2002) reported the molecular weight of chitosan extracted from four species of filamentous fungi namely, *Aspergillus niger, Rhizopus oryzae, Lentinus edodes* and *Pleurotus sajo-caju*, and two strains of yeast namely, *Zygosaccharomyces rouxii* and *Candida albicans* in the range of 2.7 X 10^4-1.9X10^5 Da. In another study, the molecular weight of chitosan extracted from *Trichoderma reesei* was reported to be 8.5 X 10^5. Our results on molecular weight analysis agree with the previous reports (29, 30) **Visual appearance of fungal chitosan -PVP blend membranes**

Visual appearance of the fungal chitosan (FC) and polyvinylpyrrolidone (PVP) blend membranes at varying composition ratios (A-F) revealed significant insights into the compatibility and filmforming characteristics of the polymer blends as shown in Fig 2. The pure fungal chitosan membrane (FC: PVP = 1:0) (Fig 2A) was yellowish-brown, opaque, brittle, and non-uniform, reflecting its rigid crystalline structure and inherent poor film-forming ability. Conversely, a commercial chitosan film (CC: PVP = 1:0) (Fig 2B) appeared more transparent and homogeneous, indicating higher purity and better solubility properties.

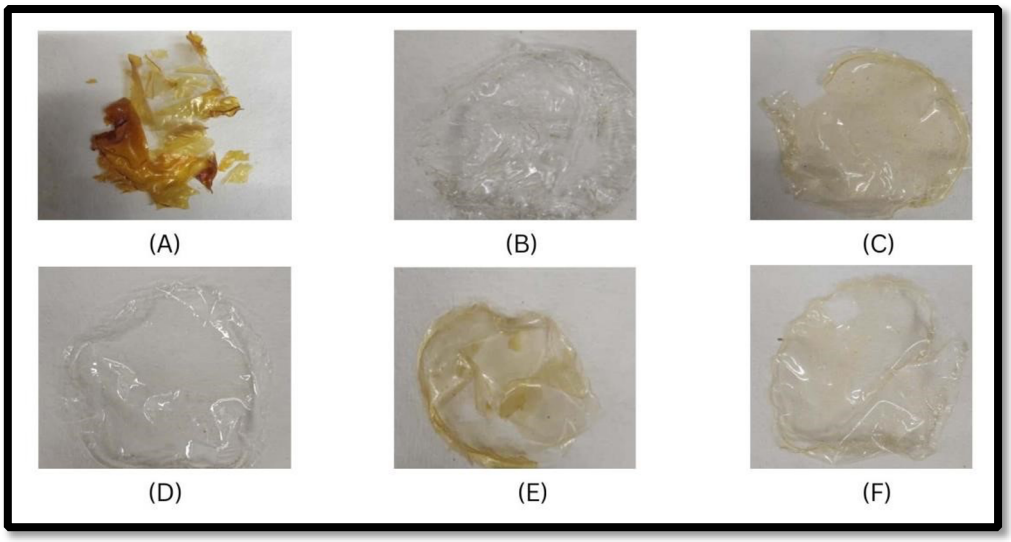

Figure 2 - FC- PVP blend membrane recovered using the solvent casting method with varying concentration

[A-FC: PVP 1:0, B-CC: PVP 1:0, C-FC: PVP 1:1, D-FC: PVP 0:1, E-FC: PVP 1:0.5, F-FC: PVP 0.5:1]

Adding PVP altered the blend membrane characteristics as well as morphology. The blend with a molar equal ratio (FC: PVP = 1:1) (Fig 2C) resulted in a smooth, semi-transparent, and flexible texture, which suggests excellent miscibility and strong intermolecular interactions. This may be attributed to the extensive hydrogen bonding between the functional groups of both polymers' fungal chitosan and PVP. The pure PVP membrane (FC: PVP = 0:1) (Fig 2D) demonstrated superior film-forming capacity, appearing highly flexible, glossy, and completely transparent, typical of its amorphous nature.

The blend with a lower PVP ratio (FC: PVP = 1:0.5) (Fig 2E) exhibited partial transparency and improved flexibility compared to pure chitosan, although a slight yellow tint suggested minor

phase heterogeneity. The blend membrane with higher PVP content (FC: PVP = 0.5:1) (Fig 2F) was almost clear, soft, and highly pliable. This signifies effective molecular blending and an improved plasticization effect (31).

Overall, with the increasing PVP content, the membranes transitioned from being brittle, opaque, and rigid to being clear, smooth, and extremely flexible. This visual evidence demonstrates that PVP serves as a plasticizer in the blend, likely improving the mechanical and optical properties of the resulting chitosan-based membranes (32).

Thickness of fungal chitosan -PVP blend membranes as determined by Screw gauge The thickness of the prepared membranes exhibited considerable variation based on the composition of the polymer blend. Table 1 represents the thickness of the FC-PVP blend membrane. The pure fungal chitosan (FC) membrane (A, 1:0 FC: PVP ratio) exhibited the smallest thickness of 0.01 mm, which can be attributed to the low intrinsic viscosity of the fungal chitosan solution or the effective packing of FC polymer chains during the evaporation of the solvent. The pure commercial chitosan (CC) membrane (B, 1:0 CC: PVP ratio) and the pure polyvinylpyrrolidone (PVP) membrane (D, 0:1 CC: PVP ratio) both demonstrated a thickness of 0.04 mm. The 1:1 FC: PVP blend membrane (C) was measured to be 0.04 mm thick, which is the same thickness as the pure CC and PVP membranes. The uniform thickness observed suggests that at this ideal stoichiometric balance, strong intermolecular hydrogen bonding between the FC and PVP chains fosters a compatible, well-ordered, and compact morphology. Conversely, membranes with non-stoichiometric ratios (E and F, specifically 1:0.5 and 0.5:1 FC: PVP, respectively) displayed a minor increase in thickness to 0.05 mm, which may indicate less dense structures relative to the 1:1 blend. These thickness variations are of considerable importance, as they directly influence the membrane's mechanical properties and mass transfer capabilities. For instance, the ultra-thin membrane A (0.01 mm) would be anticipated to have a higher flux compared to the thicker membranes (0.04 - 0.05 mm).

Table 1: Thickness of FC-PVP blends membrane

Blend Membrane Ratio (Molar ratio)	Thickness (mm)
A- FC: PVP 1:0	0.01 mm
B- CC: PVP 1:0	0.04 mm

C- FC: PVP 1:1	0.04 mm
D- FC: PVP 0:1	0.04 mm
E- FC: PVP 1:0.5	0.05 mm
F- FC: PVP 0.5:1	0.05 mm

FTIR Analysis of Fungal Chitosan-PVP Blend Membranes

The FTIR spectra of pure fungal chitosan (FC), commercial chitosan (CC), and FCS: PVP blend membranes at different molar ratios are shown in Fig 3. The FTIR spectra were analyzed to identify the functional groups, molecular interactions and peak shifts in FC-PVP in blend membranes (Table 2).

The spectrum of pure fungal chitosan (FC: PVP 1:0) (Fig 3A) exhibits characteristic absorption bands at ~3420 cm^{-1} corresponding to the stretching vibration of overlapping -OH and -NH_2 groups, ~2920 cm^{-1} assigned to C-H stretching, ~1650 cm^{-1} (amide I, C=O stretching), ~1590 cm^{-1} (N-H bending, amide II), and ~1080 cm^{-1} associated with C-O-C stretching vibrations of the polysaccharide backbone. In chitosan, these bands confirm the presence of typical chitosan functional groups, reflecting its semi-crystalline polysaccharide structure (33).

The PVP (CC: PVP 1:0) spectrum (Fig 3B) displays a strong and sharp band around 1655 cm^{-1}. This band is associated with the C=O stretching vibration of the pyrrolidone ring in the PVP structure. Furthermore, a broad band appears near 3400 cm^{-1}, which corresponds to N-H stretching vibrations. These spectral characteristics are typical of PVP and serve as a reference point for assessing possible interactions with chitosan.

In the FC: PVP blend membranes (Figs 3C-F), distinct spectral changes are observed in comparison to the commercial chitosan, indicating molecular interactions between FC and PVP.

The broad absorption band observed around 3400 cm^{-1} broadens and experiences a slight shift toward lower wave numbers with increasing PVP content. This observation implies the formation of intermolecular hydrogen bonds, specifically between the hydroxyl and amino groups of chitosan and the carbonyl group of PVP (34). Furthermore, the amide I band, approximately at 1650 cm^{-1}, diminishes in intensity and undergoes a minor shift, which suggests that chitosan and PVP interact through hydrogen bonding or dipole-dipole interactions.

Table 2: FTIR Peak Positions and Corresponding Shifts in FC-PVP blends membrane

Functional Group	Assigned	Pure Component Peak (cm^{-1})	Composite Peak (cm^{-1})	Shift (cm^{-1})	Interpretation
-OH /-NH stretch	Hydrogen bonding region	3350	3280	70	Broadening and shift indicate hydrogen bonding between chitosan and PVP
C=O stretch (PVP)	Carbonyl group	1655	1635	20	Interaction with –NH/–OH groups suggest intermolecular bonding
N–H bending (amide II)	Amine/amide	1550	1535	15	Confirms involvement of amine groups in hydrogen bonding
C–O–C stretch	Polysaccharide	1080	1055	25	Indicates structural modification due to blending
CH_2/CH_3 stretching	Alkyl groups	2920	2895	25	Slight shift reflects changes in molecular environment

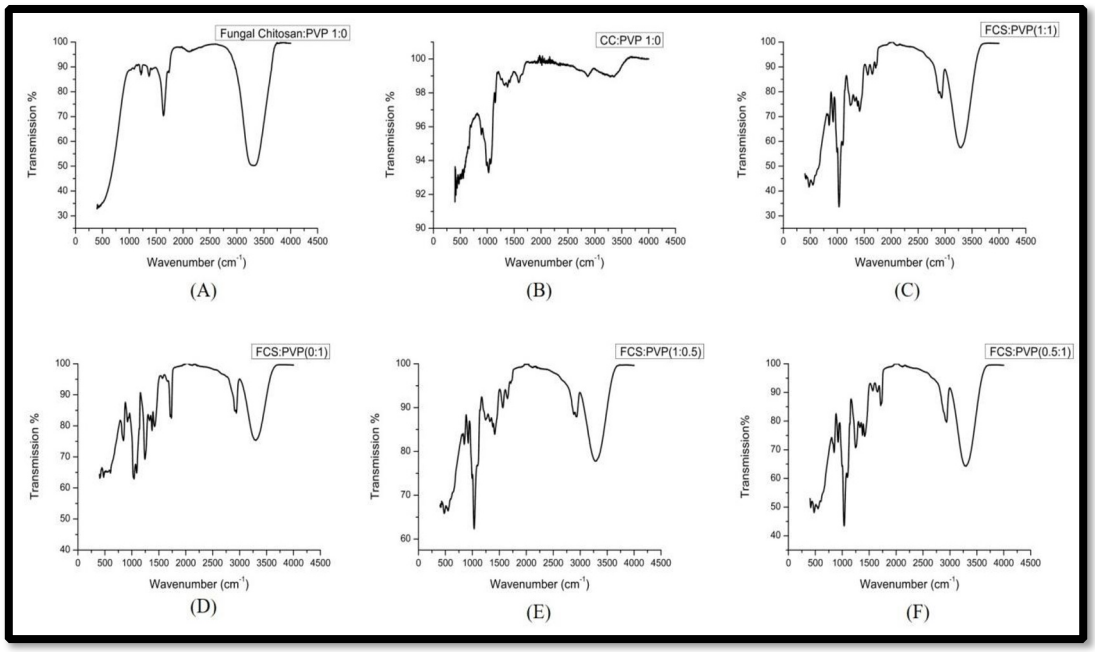

Fig 3. FTIR Spectra of FC-PVP blend membranes.
[A-FC: PVP 1:0, B-CC: PVP 1:0, C-FC: PVP 1:1, D-FC: PVP 0:1, E-FC: PVP 1:0.5, F-FC: PVP 0.5:1]

The FCS: PVP (1:1) and FCS: PVP (0.5:1) membranes (Fig 3C and 3F) show a wider absorption spectrum between 3200–3500 cm^{-1} and a less intense amide I peak. This suggests improved compatibility and stronger interactions between the polymers. The reduced intensity of the characteristic peaks indicates increased amorphous behavior, which is consistent with the XRD findings (35).

X-ray Diffraction (XRD) Analysis of Fungal Chitosan–PVP Membranes

The XRD patterns for fungal chitosan (FC), commercial chitosan, and FC: PVP blend membranes at different molar ratios are shown in Fig 4. The diffractogram for pure fungal chitosan (Fig 4A) shows two main crystalline peaks at about $2\theta = 10°$ and 20°, indicating chitosan semi-crystalline structure. These peaks represent the crystalline forms of chitosan, both with and without water. The observed reflections clearly indicate that the fungal chitosan has a well-defined crystalline structure, similar to that of commercial chitosan (Fig 4B). In comparison to commercial chitosan, the reflections are slightly sharper, suggesting a higher degree of crystallinity.

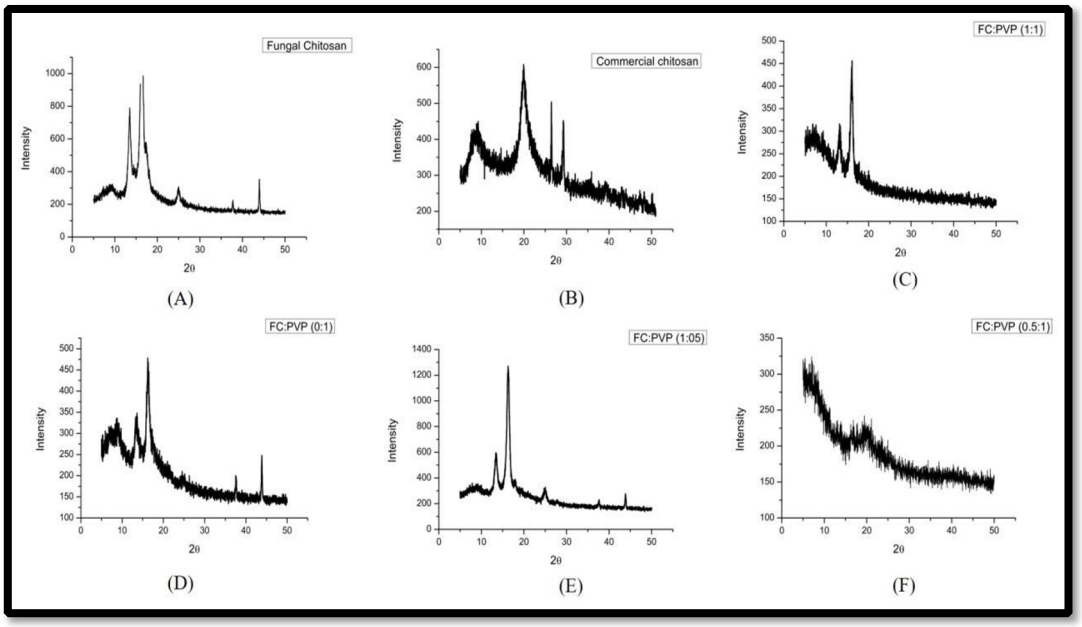

Fig 4-XRD of FC-PVP blend membranes.

[A-FC: PVP 1:0, B-CC: PVP 1:0, C-FC: PVP 1:1, D-FC: PVP 0:1, E-FC: PVP 1:0.5), F-FC: PVP 0.5:1]

The FC: PVP blend membranes (Figs 4C-F) shows significantly change in peak intensity and morphology as the polymer ratios are varied, indicating structural interactions between FC and PVP. The distinctive crystalline peaks of chitosan decrease in intensity and broaden with higher PVP concentrations, which implies a reduction in crystallinity stemming from the disruption of intermolecular hydrogen bonds within the chitosan chains. This amorphization effect, which results in a more homogeneous and amorphous polymer network, is attributed to the formation of novel hydrogen bonds between the carbonyl group of PVP and the hydroxyl and amino groups of chitosan.

The FC: PVP (1:1) and FC: PVP (0.5:1) samples (Figs. 4C and 4F) exhibit broad, less intense peaks, suggesting an increased amorphous character. The FC: PVP (1:0) sample (Fig. 4D), which consists solely of fungal chitosan, retains clear crystalline peaks. The FC: PVP (1:0.5) sample (Fig. 4E) exhibits a discernible increase in intensity at $2\theta \approx 17°$, indicating molecular rearrangement or partial recrystallization at this particular blending ratio.

The crystallinity index of each membrane was calculated using Segal's equation (eq. 3) (36).

$$CI(\%) = I_{max} - I_{am}/I_{max} \times 100 \ldots\ldots\ldots\ldots\ldots\ldots\ldots 3$$

Whereas- I_{max} is maximum intensity of crystalline peak

I_{am} is intensity of amorphous region

Crystallinity index of all blend membranes was calculated using equation 3, as shown in Table 3.

Table 3: Crystallinity ratio of FC-PVP blend membranes

Graph	Sample	Main Peak (2θ°)	I_{max}	I_{am}	CrI (%)
A	FC: PVP (1:0)	17	980	260	73.5
B	CC: PVP (0:1)	20	610	330	45.9
C	FC: PVP (1:1)	16	455	240	47.3
D	FC: PVP (0:1)	17	470	260	44.7
E	FC: PVP (1:0.5)	17	1260	300	76.2
F	FC: PVP (0.5:1)	16	340	300	53.1

Differential Scanning Calorimetry (DSC) Analysis of Fungal Chitosan–PVP Membranes The DSC thermograms, shown in Fig 5, illustrate the thermal behaviors of fungal chitosan (FC), commercial chitosan (CC), and FC: PVP blend membranes, assessed at various molar ratios. DSC serves as a valuable tool for determining the thermal characteristics and stability of polymers and their composites. This method facilitates the identification of structural changes and molecular interactions that occur with the incorporation of polyvinylpyrrolidone (PVP).

All the membranes displayed unique thermal profiles across the temperature spectrum of 0 to 500 °C (Table 4). The fungal chitosan membrane, however, demonstrated diminished stability at its glass transition temperature (T_g), suggesting its unsuitability for the autoclave conditions necessary for sterilization. The thermogram of pure fungal chitosan (Fig 5A) displays two significant endothermic transitions. The initial temperature range of 90-120 °C is associated with the loss of physically adsorbed and bound water molecules, a typical feature of hydrophilic polysaccharides (37). The second, more extensive endothermic peak, which appeared between 250 and 280 °C, indicates the thermal breakdown and partial deacetylation of the chitosan polymer. The significance of this transition supports the semi-crystalline structure of fungal chitosan, a finding that is consistent with the XRD data. Commercial chitosan (Fig 5B) exhibits similar transitions, albeit with reduced intensity, indicating variations in molecular weight or degree of deacetylation

(38).

The thermograms for the FC: PVP blend membranes (Figs 5C-F) indicate notable alterations in peak intensity and position relative to pure chitosan, thereby confirming the presence of molecular interactions between FC and PVP. The FC: PVP (1:1) sample, as depicted in Fig. 5C, displays an endothermic peak that is both broadened and shifted within the 100-150 °C interval. This observation implies enhanced water retention, which can be ascribed to hydrogen bonding interactions between the amino and hydroxyl groups present in chitosan and the carbonyl groups of PVP. Furthermore, the degradation peak is observed at elevated temperatures, specifically within the 300-350 °C range, thereby signifying an increase in the thermal stability of the blended system (39).

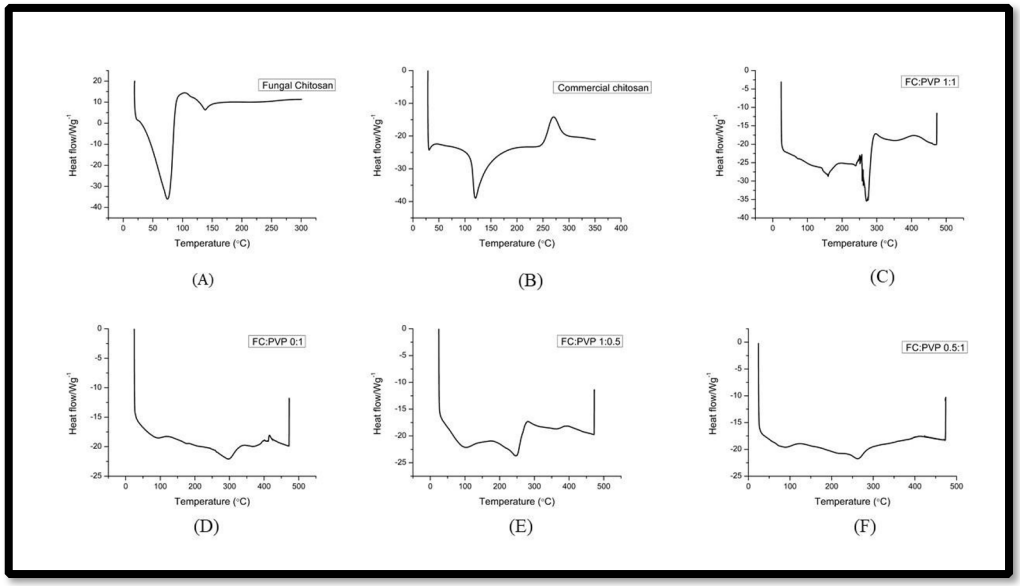

Fig. 5 DSC thermograms of FC-PVP blend membranes.
[A-FC: PVP 1:0, B-CC: PVP 1:0, C-FC: PVP 1:1, D-FC: PVP 0:1, E-FC: PVP 1:0.5), F-FC: PVP 0.5:1]

Table 4: Determination of T_g and T_m from DSC thermogram of FC-PVP blend membranes

Graph	Sample	T_g (°C)	T_m (°C)	Thermal implication
A	FC: PVP (1:0)	40°C	80°C	Low T_g indicates high chain mobility and moisture sensitivity
B	CC: PVP (0:1)	45°C	120°C	Slightly higher thermal resistance than FC
C	FC: PVP (1:1)	60°C	300°C	Improved stability due to polymer interaction
D	FC: PVP (0:1)	45°C	270°C	Moderate improvement in thermal resistance

E	FC: PVP (1:0.5)	55°C	280°C	Strong intermolecular interaction between FC and PVP
F	FC: PVP (0.5:1)	70°C	260°C	Highest T_g due to higher PVP content

The FC: PVP (1:0.5) and FC: PVP (0.5:1) samples (Fig. 5 E and 5 F) exhibit reduced enthalpy changes and broader peaks, suggesting a more amorphous and homogeneous structure compared to the pure components. The suppression or disappearance of sharp crystalline transitions further supports the partial miscibility of FC and PVP, as also evidenced by the FTIR and XRD analyses (40).

Conclusion

The combined results from X-ray diffraction (XRD), Fourier-transform infrared (FTIR) spectroscopy, and differential scanning calorimetry (DSC) analyses successfully confirm the formation of compatible and homogeneous fungal chitosan-PVP (FC: PVP) blend membranes derived from *T. reesei* MTCC 4876. The observed physical membrane thickness, ranging from 0.01 mm for pure FC to a consistent 0.04-0.05 mm for the various blends, was found to be directly influenced by this composition-dependent structural rearrangement. XRD analysis revealed a progressive shift from a semi-crystalline to a predominantly amorphous structure as the PVP content increased. This transformation is ascribed to the amorphous PVP matrix capacity to effectively disrupt chitosan inherent crystalline structure. FTIR spectroscopy confirmed the formation of robust intermolecular hydrogen bonds between the chitosan hydroxyl and amino groups and PVP carbonyl groups, as evidenced by significant shifts and broadening of the characteristic absorption bands. These strong chemical interactions are, in essence, responsible for the improved molecular-level miscibility, structural homogeneity, and the observed alterations in film density and thickness. DSC results indicated that the blends exhibited enhanced thermal stability and diminished crystallinity relative to pure chitosan, thereby validating the formation of a stable, compatible polymer network. These observations collectively suggest that combining fungal chitosan with PVP effectively modifies its structure, chemical makeup, and thermal properties. These enhancements lead to membranes that are more flexible, stable, and versatile, making them suitable for use in biomedical, pharmaceutical, and packaging settings.

Acknowledgements: The authors are grateful to the Department of Biotechnology and the Department of Physics and Materials Science and Engineering, Jaypee Institute of Information Technology, Noida, Uttar Pradesh, India, for providing the necessary facilities to execute this work.

Funding: The authors did not receive support from any organization for the submitted work.

Declarations

Conflict of interest -The authors declare that they have no conflict of interest in the publication. Competing interests- The authors have no financial and non-financial competing interests to declare that are relevant to the content of this article.

Reference

(1) Rattanaanothaikul, N., Boonyarattanakalin, K., Songnuy, T., Pecharapa, W., & Mekprasart, W. (2025). Effect of chitosan loading on structural and physical properties of polyvinylpyrrolidone/chitosan composites using simple casting process. *Creative Science*, *17*(2), 260988. https://doi.org/10.55674/cs.v17i2.260988

(2) Ulu, A., Noma, S. a. A., Gurses, C., Koytepe, S., & Ates, B. (2018). Chitosan/Polyvinylpyrrolidone/MCM-41 Composite hydrogel films: structural, thermal, surface, and antibacterial properties. *Starch - Stärke*, *70*(11–12). https://doi.org/10.1002/star.201700303 (3) Julkapli, N. M., Akil, H. M., & Ahmad, Z. (2011). Preparation, Properties and Applications of Chitosan-Based Biocomposites/Blend Materials: A review. *Composite Interfaces*, *18*(6), 449–507. https://doi.org/10.1163/156855411x610232

(4) Abdelrazek, E. M., Elzayat, A. M., Elbana, A. A., & Awad, W. M. (2023). Physical properties of copper oxide nano-composite incorporated PVP/chitosan blend matrix by casting method. *Polymer Bulletin*, *81*(8), 7467–7479. https://doi.org/10.1007/s00289-023-05052-5

(5) Spoială, A., Ilie, C., Ficai, D., Ficai, A., & Andronescu, E. (2021). Chitosan-Based Nanocomposite Polymeric Membranes for Water Purification—A Review. *Materials*, *14*(9), 2091. https://doi.org/10.3390/ma14092091

(6) Rao, K. M., Sudhakar, K., Suneetha, M., Won, S. Y., & Han, S. S. (2021). Fungal-derived carboxymethyl chitosan blended with polyvinyl alcohol as membranes for wound dressings. *International Journal of Biological Macromolecules*, *190*, 792–800. https://doi.org/10.1016/j.ijbiomac.2021.09.034

(7) Iman, H. N., Susilo, H., Satriyatama, A., Budi, I. D. M., Kurnia, K. A., Wenten, I. G., & Khoiruddin, K. (2024b). Separation properties and fouling resistance of polyethersulfone membrane modified by fungal chitosan. *BMC Chemistry*, *18*(1), 224. https://doi.org/10.1186/s13065-024-01341-w

(8) Tahir, M., Vicini, S., Jędrzejewski, T., Wrotek, S., & Sionkowska, A. (2024b). New composite materials based on PVA, PVP, CS, and PDA. *Polymers*, *16*(23), 3353. https://doi.org/10.3390/polym16233353

(9) Alrobea, H., Khan, A., Alamry, K. A., & Hussein, M. A. (2024). Antibacterial evaluation of polyvinyl alcohol/polyvinyl pyrrolidone/chitosan nanocomposite embedded curcumin@ zinc oxide. *Results in Chemistry*, *10*, 101729. https://doi.org/10.1016/j.rechem.2024.101729

(10) Sangeetha, M. S., Kandaswamy, A., & Vijayalakshmi, A. (2016). Preparation and characterisation of flat sheet micro/nanoporous membranes using polysulfone blend with PVP/PEG and chitosan/chitosan nanoparticles for biomedical applications. *J. Optoelectron. Biomed. Mater*, *8*, 81-87.

(11) Rinaudo, M. (2006). Chitin and chitosan: Properties and applications. *Progress in Polymer Science*, *31*(7), 603–632. https://doi.org/10.1016/j.progpolymsci.2006.06.001

(12) Pillai, C., Paul, W., & Sharma, C. P. (2009). Chitin and chitosan polymers: Chemistry, solubility and fiber formation. *Progress in Polymer Science*, *34*(7), 641–678. https://doi.org/10.1016/j.progpolymsci.2009.04.001

(13) Milewska, S., Niemirowicz-Laskowska, K., Siemiaszko, G., Nowicki, P., Wilczewska, A. Z., & Car, H. (2021). Current trends and challenges in pharmacoeconomic aspects of nanocarriers as drug delivery systems for cancer treatment. *International Journal of Nanomedicine*, *Volume 16*, 6593–6644. https://doi.org/10.2147/ijn.s323831

(14) Zeng, M., Zhang, L., & Kennedy, J. F. (2005). Intermolecular interaction and properties of cross-linked materials from poly(ester-urethane) and nitrochitosan. *Carbohydrate Polymers*, *60*(3), 399–409. https://doi.org/10.1016/j.carbpol.2005.02.002

(15) Kurita, K. (2006). Chitin and Chitosan: Functional Biopolymers from Marine Crustaceans. *Marine Biotechnology*, *8*(3), 203–226. https://doi.org/10.1007/s10126-005-0097-5 (16) Synowiecki, J., & Al-Khateeb, N. A. (2003). Production, properties, and some new applications of Chitin and its derivatives. *Critical Reviews in Food Science and Nutrition*, *43*(2), 145–171. https://doi.org/10.1080/10408690390826473

(17) Aranaz, I., Mengibar, M., Harris, R., Panos, I., Miralles, B., Acosta, N., Galed, G., & Heras, A. (2009). Functional characterization of Chitin and Chitosan. *Current Chemical Biology*, *3*(2), 203–230. https://doi.org/10.2174/187231309788166415

(18) Salehiabar, M., Nosrati, H., Javani, E., Aliakbarzadeh, F., Manjili, H. K., Davaran, S., & Danafar, H. (2018). Production of biological nanoparticles from bovine serum albumin as controlled release carrier for curcumin delivery. *International Journal of Biological Macromolecules*, 115, 83–89. https://doi.org/10.1016/j.ijbiomac.2018.04.043

(19) Dash, M., Chiellini, F., Ottenbrite, R., & Chiellini, E. (2011). Chitosan—A versatile semisynthetic polymer in biomedical applications. *Progress in Polymer Science*, *36*(8), 981–1014. https://doi.org/10.1016/j.progpolymsci.2011.02.001

(20) De G Sampaio, C., Frota, L. S., Magalhães, H. S., Dutra, L. M., Queiroz, D. C., Araújo, R. S., Becker, H., De Souza, J. R., Ricardo, N. M., & Trevisan, M. T. (2015). Chitosan/mangiferin particles for Cr (VI) reduction and removal. *International Journal of Biological Macromolecules*, *78*, 273–279. https://doi.org/10.1016/j.ijbiomac.2015.03.038

(21) Yen, M. T., & Mau, J. L. (2007). Physico-chemical characterization of fungal chitosan from shiitake stipes. *LWT-Food Science and Technology*, *40*(3), 472-479. https://doi.org/10.1016/j.lwt.2006.01.002

(22) Duarte, W. F., Dias, D. R., Oliveira, J. M., Teixeira, J. A., De Almeida E Silva, J. B., & Schwan, R. F. (2010). Characterization of different fruit wines made from cacao, cupuassu, gabiroba, jaboticaba and umbu. *LWT*, *43*(10), 1564–1572. https://doi.org/10.1016/j.lwt.2010.03.010

(23) Bisaria, H., Gupta, M., Shandilya, P., & Srivastava, R. (2015). Effect of fibre length on mechanical properties of randomly oriented short jute fibre reinforced epoxy composite. *Materials Today Proceedings*, *2*(4–5), 1193–1199. https://doi.org/10.1016/j.matpr.2015.07.031

(24) Kim, U., Wada, M., & Kuga, S. (2004). Solubilization of dialdehyde cellulose by hot water. *Carbohydrate Polymers*, *56*(1), 7–10. https://doi.org/10.1016/j.carbpol.2003.10.013

(25) Raza, M. A., Shahzad, K., Purohit, S. D., Park, S. H., & Han, S. S. (2023). The fabrication strategies for chitosan/poly(vinyl pyrrolidone) based hydrogels and their biomedical applications: A focused review. *Polymer-Plastics Technology and Materials*, *62*(16), 2255–2271. https://doi.org/10.1080/25740881.2023.2252928

(26) Rahman, R. U., & Mathur, G. (2025). Biotechnological production of chitosan: extraction and characterization from *Trichoderma* sp. *Biopolymers and Cell*, *41*(2), 100. https://doi.org/10.7124/bc.000b13

(27) Wu, S., Li, K., Shi, W., & Cai, J. (2022). Preparation and performance evaluation of chitosan/polyvinylpyrrolidone/polyvinyl alcohol electrospun nanofiber membrane for heavy metal ions and organic pollutants removal. International Journal of Biological Macromolecules, 210, 76–84. https://doi.org/10.1016/j.ijbiomac.2022.04.232

(28) Kabir, M. T., Kabir, M. S., Miah, A. B., Sarker, M. a. K., & Pramanik, M. K. (2020). Physicochemical Properties of Chitosan Extracted from *Pleurotus ostreatus* and Improvement of its Antibacterial Activity by Gamma Radiation. *Bangladesh Journal of Microbiology*, *37*(2), 52–55. https://doi.org/10.3329/bjm.v37i2.51211

(29) Pochanavanich, P., & Suntornsuk, W. (2002). Fungal chitosan production and its characterization. *Letters in Applied Microbiology*, *35*(1), 17–21. https://doi.org/10.1046/j.1472-765x.2002.01118.x

(30) Dhanashree G, Basavaraj H (2020). Green synthesis of Fungal Chitin and Chitosan and their Characterization Studies. *Research Journal of Chemistry and Environment*, 24 (2) 1-13.

(31) Ramadan, R., & Ismail, A. M. (2023). Structural and physical comparison between CS/PVP Blend and CS/PVP/SR-Hexaferrite nanocomposite films. *Journal of Inorganic and Organometallic Polymers and Materials*, *33*(8), 2506–2516. https://doi.org/10.1007/s10904-02302684-y

(32) Kumar, R., Ranwa, S., & Kumar, G. (2019). Biodegradable flexible substrate based on Chitosan/PVP blend polymer for disposable electronics device applications. *The Journal of Physical Chemistry B*, *124*(1), 149–155. https://doi.org/10.1021/acs.jpcb.9b08897

(33) Rhim, J., Hong, S., Park, H., & Ng, P. K. W. (2006). Preparation and Characterization of Chitosan-Based Nanocomposite Films with Antimicrobial Activity. *Journal of Agricultural and Food Chemistry*, *54*(16), 5814–5822. https://doi.org/10.1021/jf060658h

(34) Pawlak, A., & Mucha, M. (2003). Thermogravimetric and FTIR studies of chitosan blends. *Thermochimica Acta*, *396*(1–2), 153–166. https://doi.org/10.1016/s0040-6031(02)005233

(35) Marsano, E., Vicini, S., Skopiǹska, J., Wisniewski, M., & Sionkowska, A. (2004). Chitosan and Poly(vinyl pyrrolidone): Compatibility and Miscibility of Blends. *Macromolecular Symposia*, *218*(1), 251–260. https://doi.org/10.1002/masy.200451426

(36) Segal, L., Creely, J. J., Martin, A. E., & Conrad, C. M. (1959). An empirical method for estimating the degree of crystallinity of native cellulose using X-ray diffractometer. *Textile Research Journal*, 29, 786–794.https://doi.org/10.1177/004051755902901003

(37) Abdelrazek, E., Elashmawi, I., & Labeeb, S. (2010). Chitosan filler effects on the experimental characterization, spectroscopic investigation and thermal studies of PVA/PVP blend

films. *Physica B Condensed Matter*, *405*(8), 2021–2027. https://doi.org/10.1016/j.physb.2010.01.095

(38) Poonguzhali, R., Basha, S. K., & Kumari, V. S. (2016). Synthesis and characterization of chitosan/poly (vinylpyrrolidone) biocomposite for biomedical application. *Polymer Bulletin*, *74*(6), 2185–2201. https://doi.org/10.1007/s00289-016-1831-z

(39) Sizílio, R., Galvão, J., Trindade, G., Pina, L., Andrade, L., Gonsalves, J., Lira, A., Chaud, M., Alves, T., Arguelho, M., & Nunes, R. (2018). Chitosan/PVP-based mucoadhesive membranes as a promising delivery system of betamethasone-17-valerate for aphthous stomatitis. *Carbohydrate Polymers*, *190*, 339–345. https://doi.org/10.1016/j.carbpol.2018.02.079

(40) Samsoen, S., Dudognon, É., Fer, G. L., Fournier, D., Woisel, P., & Affouard, F. (2024). Impact of the polymer dispersity on the properties of curcumin/polyvinylpyrrolidone amorphous solid dispersions. *International Journal of Pharmaceutics*, *653*, 123895. https://doi.org/10.1016/j.ijpharm.2024.123895